Atmos. Chem. Phys. Discuss., https://doi.org/10.5194/acp-2018-499
Manuscript under review for journal Atmos. Chem. Phys.
Discussion started: 19 June 2018

Atmospheric Chemistry and Physics Discussions

Evaluate autoconversion and accretion enhancement factors in GCM warm-rain parameterizations using ground-based measurements at the Azores

Peng Wu[1], *Baike Xi[1], Xiquan Dong[1], and Zhibo Zhang[2]

[1] Department of Hydrology and Atmospheric Sciences, The University of Arizona, Tucson, Arizona, USA

[2] Physics Department, The University of Maryland, Baltimore County, Maryland, USA

Submitted to Atmospheric Chemistry and Physics (May 17, 2018)

Keywords: MBL clouds, enhancement factors, autoconversion and accretion processes

* Corresponding author address: Dr. Baike Xi, Department of Hydrology and Atmospheric Sciences, University of Arizona, 1133 E. James E. Rogers Way, Tucson, AZ 85721-0011. baike@email.arizona.edu; Phone: 520-626-8945

Abstract

A great challenge in climate modelling is how to parametrize sub-grid cloud processes, such as autoconversion and accretion in warm rain formation. In this study, we use ground-based observations and retrievals over the Azores to investigate the so-called enhancement factors, E_{auto} and E_{accr}, which are often used in climate models to account for the influences of sub-grid variances of cloud and precipitation water on the autoconversion and accretion processes. E_{auto} and E_{accr} are computed at a variety of tempo-spatial scales corresponding to different model resolutions. The calculated E_{auto} increase from 1.79 (0.5-hr/36 km) to 3.15 (3.5-hr/126 km), and the calculated E_{accr} increases from 1.25 (0.5-hr/36 km) to 1.6 (5-hr/180 km). Comparing the prescribed enhancement factors to the values from observations shows that GCMs are using a much higher E_{auto} (3.2) and lower E_{accr} (1.07). This helps to explain why most of the GCMs produce too frequent precipitation events but with too light precipitation intensity. The ratios of rain to cloud liquid water at E_{accr}=1.07 and E_{accr}=2.0 are 0.048 and 0.119, respectively, further proving that the prescribed value of E_{accr}=1.07 used in GCMs is too small to simulate correct precipitation intensity. Both E_{auto} and E_{accr} increase when the boundary layer becomes less stable, and the values are larger in precipitating clouds (CLWP>75 gm^{-2}) than those in nonprecipiting clouds (CLWP<75 gm^{-2}). Therefore, the selection of E_{auto} and E_{accr} values in GCMs should be regime-dependent.

Atmos. Chem. Phys. Discuss., https://doi.org/10.5194/acp-2018-499
Manuscript under review for journal Atmos. Chem. Phys.
Discussion started: 19 June 2018

1. Introduction

Due to their vast areal coverage (Warren et al., 1986, 1988; Hahn and Warren, 2007) and strong radiative cooling effect (Hartmann et al., 1992; Chen et al., 2000), small changes in the coverage or thickness of marine boundary layer (MBL) clouds could change the radiative energy budget significantly (Hartmann and Short, 1980; Randall et al., 1984) or even offset the radiative effects produced by increasing greenhouse gases (Slingo, 1990). The lifetime of MBL clouds remains an issue in climate models (Yoo and Li, 2012; Jiang et al., 2012; Yoo et al., 2013; Stanfield et al., 2014) and represents one of the largest uncertainties in predicting future climate (Wielicki et al., 1995; Houghton et al., 2001; Bony and Dufresne, 2005).

MBL clouds frequently produce precipitation, mostly in the form of drizzle (Austin et al., 1995; Wood, 2005a; Leon et al., 2008; Wood, 2012). A significant amount of drizzle are evaporated before reaching the surface, for example, about ~76% over the Azores region in Northeast Atlantic (Wu et al., 2015), which provides another water vapour source for MBL clouds. Due to their pristine environment and their close vicinity to the surface, MBL clouds are especially sensitive to aerosol perturbations and constitute the central piece of global aerosol indirect effects in climate models (Quaas et al., 2009; Kooperman et al., 2012). Most aerosol indirect effects are associated with precipitation suppression (Albrecht, 1989; Ackerman et al., 2004; Lohmann and Feichter, 2005; Wood, 2007). Thus, accurate prediction of precipitation is essential in simulating the global energy budget and in constraining aerosol indirect effects in climate projections.

Due to the coarse spatial resolutions of the general circulation model (GCM) grid, many cloud processes cannot be adequately resolved and must be parameterized (Morrison and Gettleman, 2008). For Example, warm rain parameterizations in most GCMs treat the condensed water as either cloud or rain in the processes of autoconversion and accretion (Kessler, 1969; Khairoutdinov and Kogan, 2000; Morrison and Gettleman, 2008). Autoconversion is the process that drizzle drops being formed through the collision-coalescence of cloud droplets and accretion is the process where rain drops grow by the coalescence of drizzle-sized drops with cloud droplets. Autoconversion mainly accounts for precipitation initiation while accretion primarily contributes to precipitation intensity. Autoconversion is often parameterized as functions of cloud droplet number concentration (N_c) and cloud water mixing ratio (q_c), while accretion depends on both cloud and rain water mixing ratios (q_c and q_r) (Kessler, 1969; Tripoli and Cotton, 1980; Beheng, 1994; Khairoutdinov and Kogan, 2000; Liu and Daum, 2004; Wood, 2005b; Morrison and Gettleman, 2008; Larson and Griffin, 2013). All the previous studies proposed that these two processes as power law functions of cloud and precipitation properties (See section 2 for details).

In conventional GCMs, the lack of information on the sub-grid variances of cloud and precipitation leads to the unavoidable use of the grid-mean quantities (N_c', q_c', and q_r', where prime denotes grid mean, same below) in calculating autoconversion and accretion rates. However, due to the nonlinear nature of the relationships and positive skewness of MBL cloud liquid water path (CLWP) distributions from measurements (Wood and Hartmann, 2006), the two processes depend significantly on the sub-grid scale variability and co-variability of cloud and precipitation microphysical properties (Weber and Quass, 2012; Boutle et al., 2014). In GCMs, sub-grid scale variability is often ignored or hard coded using constants to represent the variabilities under all meteorological conditions and across the entire globe (Pincus and Klein, 2000; Morrison and Gettleman, 2008; Lebsock et al. 2013). This could lead to systematic errors in precipitation rate simulations (Wood et al., 2002; Larson et al., 2011; Lebsock et al. 2013; Boutle et al., 2014; Song et al. 2018), where GCMs are found to produce too frequent but too light precipitation compared to observations (Zhang et al., 2002; Jess, 2010; Stephens et al., 2010; Nam and Quaas, 2012; Song et al. 2018). The bias is found to be smaller by using a probability density function (PDF) of cloud water to represent the sub-grid scale variability in autoconversion parameterization (Beheng, 1994; Zhang et al., 2002; Jess, 2010), or more complexly, by integrating the autoconversion rate over a joint PDF of liquid water potential temperature, vertical velocity, total water mixing ratio and rain water mixing ratio (Cheng and Xu, 2009).

Process rate enhancement factors (*E*) are introduced when considering sub-grid scale variability in parameterizing grid-mean processes and they should be parameterized as functions of the PDFs of cloud and precipitation properties within a grid box (Morrison and Gettleman, 2008; Lebsock et al. 2013; Boutle et al., 2014). However, these values in GCMs are prescribed as constants regardless of underlying surface or meteorological conditions (Xie and Zhang, 2015). Previous studies used aircraft *in situ* measurements (Boutle et al., 2014) and satellite observations (Lebsock et al. 2013) to evaluate the dependence of *E* on sub-grid scale variability over oceans. These studies found that sub-grid scale variability and covariance between cloud and precipitation properties significantly affect autoconversion and accretion parameterizations. Using ground-based observations and retrievals, Xie and Zhang (2015) proposed a scale-aware cloud inhomogeneity parameterization that they applied to the Community Earth System Model (CESM) and found that it can recognize spatial scales without manual tuning. The inhomogeneity parameter is essential in calculating enhancement factors and affect the conversion rate from cloud to rain liquid. Xie and Zhang (2015), however, did not evaluate the validity of CESM simulations from their parameterization; the effect of N_c variability, or the effect of covariance of cloud and rain on accretion process was not assessed.

Dong et al. (2014a and 2014b) and Wu et al. (2015) reported MBL cloud and drizzle properties over the Azores and provided the possibility of calculating the enhancement

Atmos. Chem. Phys. Discuss., https://doi.org/10.5194/acp-2018-499
Manuscript under review for journal Atmos. Chem. Phys.
Discussion started: 19 June 2018

Atmospheric Chemistry and Physics Discussions
Open Access
EGU

factors using ground-based observations and retrievals. This manuscript is organized as follows: section 2 will include a summary of the mathematical formulas from previous studies that can be used to calculate grid-mean process enhancement factors. Ground-based observations and retrievals are introduced in Section 3. Section 4 presents results and discussion, followed by summary and conclusions in Section 5.

2. Mathematical Background

Autoconversion and accretion rates in GCMs are usually parameterized as power law equations (Tripoli and Cotton, 1980; Beheng, 1994; Khairoutdinov and Kogan, 2000; Liu and Daum, 2004; Morrison and Gettleman, 2008):

$$\left(\frac{\partial q_r}{\partial t}\right)_{auto} = A q_c'^{a1} N_c'^{a2}, \qquad (1)$$

$$\left(\frac{\partial q_r}{\partial t}\right)_{accr} = B(q_c' q_r')^{b}, \qquad (2)$$

where A, $a1$, $a2$, B, and b are constants that change value depending on which scheme is being used. Table 1 provides a list of the schemes and their associated constants. q_c', q_r', and N_c' are grid-mean cloud water mixing ratio, rain water mixing ratio, and droplet number concentration, respectively. Because it is widely used in model parameterizations, the detailed results from Khairoutdinov and Kogan (2000) and Morrison and Gettleman (2008) scheme will be shown in Section 4 while a summary will be given for other schemes.

Ideally, the covariance between physical quantities should be considered in the calculation of both processes. However, q_c' and N_c' in Eq. (1) are arguably not independently retrieved in our retrieval method which will be introduced in the section below. We only assess the individual roles of q_c and N_c sub-grid variations in determining autoconversion rate. q_c and q_r, on the other hand, are retrieved from two independent algorithms as shown in Dong et al. (2014a and 2014b) and Wu et al. (2015), thus we will assess the effect of cloud and rain property covariance on accretion rate calculations.

In the sub-grid scale, the PDFs of q_c and N_c are assumed to follow a gamma distribution based on observational studies of optical depth in MBL clouds (Barker et al., 1996; Pincus et al., 1999; Wood and Hartmann, 2006):

$$P(x) = \frac{\alpha^{\nu}}{\Gamma(\nu)} x^{\nu-1} e^{-\alpha x} , \quad (3)$$

where x represents q_c or N_c with grid-mean quantity q_c' or N_c', represented by μ, $\alpha = \nu/\mu$ is the scale parameter, σ^2 is the relative variance of x (= variance divided by μ^2), $\nu = 1/\sigma^2$ is the shape parameter. ν is an indicator of cloud field homogeneity, with large values representing homogeneous and small values indicating inhomogeneous cloud fields.

By integrating autoconversion rate, Eq. (1), over the grid-mean rate, Eq. (3), with respect to sub-grid scale variation of q_c and N_c, the autoconversion rate can be expressed as:

$$\left(\frac{\partial q_r}{\partial t}\right)_{auto} = A\mu_{q_c}^{2.47}\mu_{N_c}^{-1.79}\frac{\Gamma(\nu+a)}{\Gamma(2.47)\nu^{a}}, \quad (4)$$

Atmos. Chem. Phys. Discuss., https://doi.org/10.5194/acp-2018-499
Manuscript under review for journal Atmos. Chem. Phys.
Discussion started: 19 June 2018

where $a = a1$ or $a2$. Comparing Eq. (4) to Eq. (1) gives the the autoconversion enhancement factors (E_{auto}) with respect to q_c and N_c:

$$E_{auto} = \frac{\Gamma(\nu+a)}{\Gamma(a)\nu^a}. \tag{5}$$

In addition to fitting the distributions of q_c and N_c, we also tried two other methods to calculate E_{auto}. The first is to integrate Eq. (1) over the actual PDFs from observed or retrieved parameters and the second is to fit a lognormal distribution for sub-grid variability like what has been done in other studies (e.g., Lebsock et al., 2013; Larson and Griffin, 2013). It is found that all three methods get similar results. In this study, we use a gamma distribution that is consistent with the widely used GCM parameterization (Morrison and Gettleman, 2008). Also note that, in the calculation of E_{auto} from N_c', the negative exponent (-1.79) may cause singularity problems in Eq. (5). When this situation occurs, we do direct calculations by integrating the N_c PDF rather than using Eq. (5).

To account for the covariance of microphysical quantities in a model grid, it is hard to apply bivariate gamma distribution due to its complex nature. In this study, the bivariate lognormal distribution of q_c and q_r is used (Lebsock et al., 2013; Boutle et al., 2014) and can be written as:

$$P(q_c', q_r') = \frac{1}{2\pi q_c' q_r' \sigma_{q_c} \sigma_{q_r} \sqrt{1-\rho^2}} exp\left\{-\frac{1}{2}\frac{1}{1-\rho^2}\left[\left(\frac{ln q_c' - \mu_{q_c}}{\sigma_{q_c}}\right)^2 - 2\rho\left(\frac{ln q_c' - \mu_{q_c}}{\sigma_{q_c}}\right)\left(\frac{ln q_r' - \mu_{q_r}}{\sigma_{q_r}}\right) + \left(\frac{ln q_r' - \mu_{q_r}}{\sigma_{q_r}}\right)^2\right]\right\}, \tag{6}$$

Atmos. Chem. Phys. Discuss., https://doi.org/10.5194/acp-2018-499
Manuscript under review for journal Atmos. Chem. Phys.
Discussion started: 19 June 2018

where σ is standard deviation and ρ is the correlation coefficient of q_c and q_r.

Similarly, by integrating the accretion rate in Eq. (2) from Eq. (6), we get the accretion enhancement factor (E_{accr}) of:

$$E_{accr} = \left(1+\frac{1}{\nu_{q_c}}\right)^{\frac{1.15^2-1.15}{2}} \left(1+\frac{1}{\nu_{q_r}}\right)^{\frac{1.15^2-1.15}{2}} \exp(\rho 1.15^2 \sqrt{\ln\left(1+\frac{1}{\nu_{q_c}}\right)\ln(1+\frac{1}{\nu_{q_r}})}). \quad (7)$$

3. Ground-based observations and retrievals

The datasets used in this study were collected at the Department of Energy (DOE) Atmospheric Radiation Measurement (ARM) Mobile Facility (AMF), which was deployed on the northern coast of Graciosa Island (39.09°N, 28.03°W) from June 2009 to December 2010 (for more details, please refer to Rémillard et al. 2012; Dong et al. 2014a and Wood et al. 2015). The detailed operational status of the remote sensing instruments on AMF was summarized in Figure 1 of Rémillard et al. (2012) and discussed in Wood et al. (2015). The ARM Eastern North Atlantic (ENA) site was established on the same island in 2013 and provides long-term continuous observations.

The cloud-top heights (Z_{top}) were determined from W-band ARM cloud radar (WACR) reflectivity and only single-layered low-level clouds with $Z_{top} \leq 3$ km are selected. Cloud-base heights (Z_{base}) were detected by a laser ceilometer (CEIL) and the cloud thickness was simply the difference between cloud top and base heights. The cloud liquid water path (CLWP) was retrieved from microwave radiometer (MWR) brightness temperatures measured at 23.8 and 31.4 GHz using a statistical retrieval method with an uncertainty of 20 g m^{-2} for CLWP < 200 g m^{-2}, and 10% for CLWP > 200 g m^{-2} (Liljegren et al., 2001; Dong et al., 2000). Drizzling status is identified through a combination of WACR reflectivity and Z_{base}. As in Wu et al. (2015), we label the status of a specific time as "drizzling" if the WACR reflectivity below the cloud base exceeds -37 dBZ.

Cloud microphysical properties (CLWC and N_c) are retrieved using the methods presented in Dong et al. (2014a and 2014b). The CLWC values are transformed to q_c when calculating autoconversion and accretion rates by dividing by air density. Drizzle property, or rain LWP, (RLWP), below Z_{base} is retrieved using the method proposed in O'Connor et al. (2005) and used by Wu et al. (2015). Similarly, drizzle LWC (DLWC) is transformed to q_r when calculating the accretion rate.

The ARM merged sounding data (Troyan, 2012) are used to calculate lower tropospheric stability (LTS), which is used to infer the boundary layer stability. In this study, unstable and stable boundary layers are defined as LTS less than 13.5 K and greater than 18 K, respectively, and environment with an LTS between 13.5 K and 18 K is defined as mid-stable (Wang et al. 2012; Bai et al. 2018). Enhancement factors in different boundary layers are summarized in Section 4.2 and may be used as references for model simulations. Further, two regimes are classified: CLWP greater than 75 g m^{-2} as precipitating and CLWP less than 75 g m^{-2} as nonprecipitating (Rémillard et al., 2012).

Atmos. Chem. Phys. Discuss., https://doi.org/10.5194/acp-2018-499
Manuscript under review for journal Atmos. Chem. Phys.
Discussion started: 19 June 2018

To evaluate the dependence of autoconversion and accretion rates on sub-grid scale variabilities for different model spatial resolutions, we use a variety of time-intervals to mimic different grid sizes. For example, a 2-hour interval corresponds to a 72-km grid box if assuming 10 $m\ s^{-1}$ horizontal wind and a 5-hour interval corresponds to a 180-km grid box. We used 10 time-intervals (0.5-, 1-, 1.5-, 2-, 2.5-, 3-, 3.5-, 4-, 4.5-, 5-hour) and mainly show the results from 2-hour and 5-hour intervals in Section 4.

4. Results and discussions

In this section, we first show the data and methods using a selected case, followed by statistical analysis based on 19-month of data and multiple time-intervals.

4.1 Case study

The selected case occurred at the Azores on July 27, 2010 (Figure 1a). This case was characterized by a long time of non-drizzling or light drizzling cloud development (00:00-14:00 UTC) before intense drizzling occurs (14:00-20:00 UTC). Wu et al. (2017) studied this case in detail to demonstrate the effect of wind shear on drizzle initiation. Here, we choose two periods with similar mean CLWPs: 81 g m^{-2} for 7:00 – 12:00 UTC (period c) and 85 g m^{-2} for 13:00 – 18:00 UTC (period d) but with different distributions (Figures 1c and 1d). The PDFs of CLWP are then fitted using gamma distributions to get shape parameters (ν) as shown in Figures 1c and 1d. Smaller ν is usually associated with more inhomogeneous cloud field, which allows more rapid drizzle production and more efficient liquid transformation from cloud to rain (Xie and Zhang, 2015) in regions that satisfy precipitation criteria, which is usually controlled using threshold q_r, droplet size or relative humidity (Kessler, 1969; Liu and Daum, 2004). The period d has a wider CLWP distribution than the period c, resulting in a smaller ν and thus larger E_{auto}. Using the fitted ν, the E_{auto} from CLWP is calculated from Eq. (5) and the period d is larger (1.81 vs. 1.33). The E_{auto} values for the periods d and c can also be calculated from N_c using the same procedure as CLWP with similar result (2.1 vs. 1.51). The E_{accr} values for the periods d and c can be calculated from the covariance of CLWP and RLWP and Eq. (7). Not surprisingly, the period d has larger E_{auto} than the period c. The combination of larger E_{auto} and E_{accr} in the period d contribute to the rapid drizzle production and high rain rate as seen from WACR reflectivity and RLWP.

It is important to clarify the meaning of enhancement factors in precipitation parameterization. If we assume two scenarios for CLWPs with a model grid having the same mean values but different distributions: (1) The distribution is extremely homogeneous, there will be no sub-grid variability because the cloud has the same chance to precipitate and the enhancement factors would be unity (this is true for arbitrary grid-mean CLWP amount as well). (2) The cloud field gets more and more inhomogeneous with a broad range of CLWPs within the model grid box, which results in a greater enhancement factor and increases the possibility of precipitation. That is, a large enhancement factor can make the part of cloud with higher CLWPs within the grid box become more efficient in generating precipitation, rather than the entire model grid.

It is clear that CLWP and N_c in Figure 1b are correlated with each other. In addition to their natural relationships, CLWP and N_c in our retrieval method are also correlated (Dong et al. 2014a and 2014b). Thus, the effect of CLWP and N_c covariance on E_{auto} is not included in this study. In Figures 1c and 1d, the results are calculated using a time-interval of 5-hour for the selected case on 27 July 2010. In Section 4.2, we will use these approaches to calculate their statistical results for multiple time-intervals using the 19-month ARM ground-based observations and retrievals.

4.2 Statistical result

For a specific time-interval, e.g. 2-hour, we estimate the shape parameter (ν) and calculate E_{auto} through Eqns. (5) and (7). The PDFs of E_{auto} for both 2-hour and 5-hour intervals are shown in Figures 2a-2d. The distributions of E_{auto} values calculated from CLWPs with 2-hour and 5-hour intervals (Figures 2a and 2b) are similar to each other with nearly the same mean values (2.95 vs. 3.16). The calculated E_{auto} values range from 1 to 10, and most are less than 4 with bi-model distributions. The average value for the 2-hour interval (2.95) is smaller than that for the 5-hour window (3.16), indicating a possible dependence of E_{auto} on model grid size. Because drizzle-sized drops are initiated from autoconversion process, we investigate the relationship of E_{auto} and precipitation frequency, which we define as the average percentage of drizzling occurrence based on radar reflectivity below cloud base. The precipitation frequency (black lines in Figures 2a and 2b) within each PDF bin shows an increasing trend for E_{auto} from 0 to ~4, then stays relatively constant when E_{auto} > 4, indicating that in precipitation initiation process, E_{auto} keeps increasing to a certain value (~4) until the precipitation frequency reaches a near-steady state. Larger E_{auto} values do not necessarily result in higher precipitation frequency but instead may produce more drizzle-sized drops from autoconversion process when the cloud is precipitating. Therefore, the E_{auto} value of 4 is a critical threshold for converting cloud droplets into drizzle drops within MBL clouds.

The PDFs of E_{auto} calculated from N_c also share similar patterns of positive skewness and peaks at ~1.5-2.0 for the 2-hour and 5-hour intervals (Figures 2c and 2d). Although the average values are close to their CLWP counterparts (2.69 vs. 2.95 for 2-hr and 3.45 vs. 3.16 for 5-hr), the difference between 2-hour and 5-hour intervals becomes large. The precipitation frequencies within each bin do not show similar slightly decreasing trend like what is shown in Figures 2a and 2b. This suggests complicated effects of droplet number concentration on precipitation initiation and warrants more explorations of aerosol-cloud-precipitation interactions. This is very intriguing result, which suggests the existence of significant sub-grid variation of N_c and this variation can significantly influence the warm rain process. As mentioned in Section 2, we also fit CLWP and N_c using lognormal distributions. The distributions of E_{auto} are close to Figure 2 (not shown here) with average values of 3.33 and 3.67, respectively, for 2-hour and 5-hour intervals.

The covariance of CLWP and RLWP (equivalently, q_c and q_r) is included in calculating E_{accr} and the results are shown in Figures 2e and 2f. The calculated E_{accr} values range from 1 to 4 with mean values of 1.48 and 1.60 for 2-hour and 5-hour intervals, respectively. These two mean values are much greater than the prescribed value used in GCMs (1.07 for example from Morrison and Gettleman, 2008). Since accretion is the process where rain drops collect cloud droplets, we superimpose the ratio of RLWP to CLWP within each bin (black lines in Figures 2e and 2f) to represent the portion of rain water in the atmospheric column. This ratio increases from E_{accr}=0 to ~2, and then decreases, suggesting a possible optimal state for collision-coalescence process to achieve maximum efficiency for converting cloud water into rain water at E_{accr}=2. In other words, the conversion efficiency cannot be infinitely increased with E_{accr} under fixed available cloud water. The ratios of RLWP to CLWP at E_{accr}=1.07 and E_{accr}=2.0 are 0.048 and 0.119, further proving that the prescribed value of E_{accr}=1.07 used in GCMs is too small to simulate correct precipitation intensity in the models. Therefore, we suggest increasing E_{accr} from 1.07 to 1.5-2.0 in GCMs.

To illustrate the impact of using prescribed enhancement factors, autoconversion and accretion rates are calculated using the prescribed values in GCMs (e.g., 3.2 for E_{auto} and 1.07 for E_{accr}, Morrison and Gettleman, 2008; Xie and Zhang, 2015) and the newly calculated ones in Figure 2 that use observations and retrievals. The q_c and q_r are calculated by dividing cloud or rain water content by air density from the merged sounding. Figure 3 shows the joint density of autoconversion (Figures 3a and 3b) and accretion rates (Figures 3c and 3d) from observations (x-axis) and model parameterizations (y-axis) for 2-hour and 5-hour intervals. Despite the spread, the peaks of the joint density of autoconversion rate appear slightly above the one-to-one line, suggesting that cloud droplets in the model are more easily to be converted into drizzle/rain drops than observations. On the other hand, the peaks of accretion rate appear slightly below the one-to-one line which indicates that simulated precipitation intensities are lower than observed ones. The magnitudes of the two rates are consistent with Khairoutdinov and Kogan (2000), Liu and Daum (2004), and Wood (2005b).

Compared to the observations, the precipitation in GCMs occurs at higher frequencies with lower intensities, which might explain why the total precipitation amounts are close to surface measurements over an entire grid-box. This ‘promising’ result, however, fails to simulate precipitation on the right time scale and cannot capture the correct rain water amount, thus providing limited information in severe weather warnings such as flash flooding.

Clouds in an unstable boundary layer have a better chance of getting moisture supply from the surface by upward motion than clouds in a stable boundary layer. Precipitation frequencies are thus different in the two boundary layer regimes. For example, clouds in a relatively unstable boundary layer seem easier to produce drizzle than those in a stable boundary layer (Wu et al., 2017). Provided the same boundary layer condition, CLWP is an important factor in determining the precipitation status of clouds. At the Azores, drizzling clouds are more likely to have CLWP greater than 75 g m^{-2} than their nondrizzling counterparts (Rémillard et al., 2012). To further investigate what conditions and parameters can significantly influence the enhancement factors, we classify low-level clouds according to their boundary layer conditions and CLWPs.

The averaged E_{auto} and E_{accr} values for each category are listed in Table 2. Both E_{auto} and E_{accr} increase when the boundary layer becomes less stable, and these values become larger in precipitating clouds (CLWP>75 gm^{-2}) than those in nonprecipiting clouds (CLWP<75 gm^{-2}). In real applications, autoconversion process only occurs when q_c or cloud droplet size reaches a certain threshold (e.g., Kessler, 1969 and Liu and Daum, 2004). Thus, it will not affect model simulations if a valid E_{auto} is assigned to Eq. (1) in a nonprecipitating cloud. The E_{auto} values in both stable and mid-stable boundary layer conditions are smaller than the prescribed value of 3.2 in GCMs, while the values in unstable boundary layers are significantly larger than 3.2 regardless of if they are precipitating or not. All E_{accr} values are greater than 1.07, the constant used in GCMs. The E_{auto} values in Table 2 range from 2.31 to 6.17 and the E_{accr} values vary from 1.4 to 1.7, depending on different boundary layer conditions and CLWPs. Therefore, the selection of E_{auto} and E_{accr} values in GCMs should be regime-dependent.

Atmos. Chem. Phys. Discuss., https://doi.org/10.5194/acp-2018-499
Manuscript under review for journal Atmos. Chem. Phys.
Discussion started: 19 June 2018

Atmospheric Chemistry and Physics Discussions

Although the difference of E_{auto} and E_{accr} between the model and the observations exist, it is difficult to vary enhancement factors for each grid box at each time step in GCM simulations. Proper adjustments, however, can be made according to the model grid size, boundary layer conditions, and precipitating status. As stated in the methodology, we used a variety of time intervals, by assuming a 10 $m\ s^{-1}$ horizontal wind, those intervals would correspond to different spatial scales implying different model resolutions. Figure 4 demonstrates the dependence of both enhancement factors on different time intervals and model grid sizes. The E_{auto} values increase from 1.79 at a grid box of 18×18 km to 3.11 at a grid box of 108×108 km, which are 44% and 3% percent lower than the value used in GCMs (3.2, upper dashed line). After that, the E_{auto} values remain relatively constant, at around 3.15, which is close to the prescribed value used in GCMs. The E_{accr} values increase from 1.25 at a grid box of 18×18 km to 1.53 at a grid box of 108×108 km, those are 17% and 43%, respectively, larger than the value used in GCMs (1.07, lower dashed line). These results suggest that the current GCMs should increase their prescribed E_{accr} value by 43% in their simulations of precipitation within a grid box of $1^{o}\times1^{o}$.

It is noted that E_{auto} and E_{accr} depart from GCM prescribed values at opposite directions as model grid size increases. For models with finer resolutions (e.g., 18 km or 54 km), both E_{auto} and E_{accr} are significantly different from the values in GCMs, which can partially explain the issue of 'too frequent' and 'too light' precipitation. Under both conditions, the accuracy of precipitation estimation is degraded. For models with coarser resolutions (e.g., 144 km or 180 km), E_{auto} is close to 3.2 while E_{accr} is much larger than 1.07 when compared to finer resolution simulations. In such situations, the simulated precipitation will be dominated by the 'too light' problem, in addition to regime-dependent (Table 2), E_{auto} and E_{accr} should be also scale-dependent.

Also note that the location we choose to collect ground-based observations and retrievals is on the remote ocean where the MBL clouds mainly form in a relatively stable boundary layer and are characterized by high precipitation frequency. Even in such environments, however, the GCMs overestimate the precipitation frequency (Ahlgrimm and Forbes, 2014). In an environment where boundary layer structures are more complicated and precipitation events occur less often, the continental US for example, using the fixed E_{auto} value would cause much larger errors than those that occur over the Azores. Therefore, for simulations over continents we suggest using E_{auto} values that are even smaller than what is suggested in Figure 4.

To further investigate how enhancement factors affect precipitation simulations, we use E_{auto} as a fixed value of 3.2 in Eq. (4), and then calculate the CLWPs needed for models to reach the same autoconversion rate as observations. The CLWP differences between models and observations are representing the amount of liquid water needed by models to adjust for getting a realistic autoconversion rate in the simulations. Similar to Figure 1, the PDFs of

CLWP differences (model – observation) are plotted in Figures 5a and 5b for 2-hour and 5-hour intervals. Figure 5c shows the average percentages of model CLWP adjustments for all time intervals, which corresponds to different model grid sizes. The mode and average values for both time intervals are negative, suggesting that models need to simulate lower CLWPs in general to get reasonable autoconversion rates. Lower CLWPs are usually associate with smaller E_{auto} values that induce lower simulated precipitation frequency. On average, the percentage of CLWP adjustments decrease with increasing model grid size. For example, the adjustments for finer resolutions (e.g., 18 – 54 km) can be more than 20% of the cloud water, whereas adjustments in coarse resolution models (e.g., 144 – 180 km) are relatively small because the prescribed E_{auto} (=3.2) is close to the values from observations (Figure 4). The adjustment method presented in Figure 5 however, changes cloud water substantially and may cause variety of subsequent issues, such as altering cloud radiative effects and disrupting the hydrological cycle. The assessment we do in Figure 5 only provides a reference to the equivalent effect on cloud water by using the prescribed E_{auto} value in GCMs as compared to those from observations.

All above discussions are based on the prescribed E_{auto} and E_{accr} values (3.2 and 1.07) in GCMs and WRF from Morrison and Gettelman (2008). Whereas there are quite a few parameterizations that have been published so far, in this study, we list E_{auto} and E_{accr} for three widely used parameterization schemes in Table 3, which are given only for 2-hour and

Atmos. Chem. Phys. Discuss., https://doi.org/10.5194/acp-2018-499
Manuscript under review for journal Atmos. Chem. Phys.
Discussion started: 19 June 2018

5-hour intervals. The values of the exponent in each scheme directly affect the values of the enhancement factors. For example, the Beheng (1994) scheme has highest degree of nonlinearity and hence has the largest enhancement factors. The Liu and Daum (2004) scheme is very similar to the Khairoutdinov and Kogan (2000) scheme because both schemes have a physically realistic dependence on cloud water content and number concentration (Wood, 2005b). For a detailed overview and discussion of various existing parameterizations, please refer to Liu and Daum (2004), Liu et al. (2006a), Liu et al. (2004b) and Wood (2005b).

5. Summary

To better understand the influence of sub-grid cloud variations on the warm-rain process simulations in GCMs, we investigated the warm-rain parameterizations of autoconversion (E_{auto}) and accretion (E_{accr}) enhancement factors. These two factors represent the effects of sub-grid cloud and precipitation variabilities when parameterizing autoconversion and accretion rates as functions of grid-mean quantities. In current GCMs, E_{auto} and E_{accr} are prescribed as 3.2 and 1.07, respectively, in the widely used Morrison and Gettleman (2008) scheme. To assess the dependence of the two parameters on sub-grid scale variabilities, we used ground-based observations and retrievals collected at DOE ARM Azores site to reconstruct the two enhancement factors in a variety of time intervals and different model grid sizes.

The calculated E_{auto} values from observations and retrievals increase from 1.79 at a grid box of 18×18 km to 3.15 at a grid box of 108×108 km. These values are 44% and 3% lower than the prescribed value of 3.2 in Morrison and Gettleman (2008) scheme. On the other hand, the E_{accr} values increase from 1.25 at a grid box of 18×18 km to 1.53 at a grid box of 108×108 km, which are 17% and 43% higher than the prescribed value (1.07). The much higher E_{auto} and lower E_{accr} prescribed in GCMs help to explain why most produce too frequent precipitation events with a precipitation intensity that is too light. The ratios of rain to cloud liquid water increase with increasing E_{accr} from 0 to 2, and then decrease after that, suggesting a possible optimal state for the collision-coalescence process to achieve maximum efficiency for converting cloud water into rain water at E_{accr}=2. The ratios of RLWP to CLWP at E_{accr}=1.07 and E_{accr}=2.0 are 0.048 and 0.119, further proving that the prescribed value of E_{accr}=1.07 used in GCMs is too small to simulate correct precipitation intensity in models.

To further investigate what conditions and parameters can significantly influence the enhancement factors, we classified low-level clouds according to their boundary layer conditions and CLWPs. Both E_{auto} and E_{accr} increase when the boundary layer conditions become less stable, and the values are larger in precipitating clouds (CLWP>75 gm^{-2}) than those in nonprecipiting clouds (CLWP<75 gm^{-2}). The E_{auto} values in both stable and mid-stable boundary layer conditions are smaller than the prescribed value of 3.2 used in GCMs, while those values in unstable boundary layers conditions are significantly larger than 3.2 regardless of whether or not the cloud is precipitating. All E_{accr} values are greater than the prescribed value of 1.07 used in GCMs. Therefore, the selection of E_{auto} and E_{accr} values in GCMs should be regime-dependent.

This study, however, did not include the effect of uncertainties in GCM simulated cloud and precipitation properties on sub-grid scale variations. For example, we did not consider the behavior of the two enhancement factors under different aerosol regimes, a condition which may affect precipitation formation process. In addition, other factors may also affect precipitation frequency and intensity even under the same aerosol regimes and even if the clouds have similar cloud water contents. Wind shear, for example as presented in Wu et al. (2017), is an external variable that can affect precipitation formation. Further studies are needed to evaluate the role of the covariance of q_c and N_c in sub-grid scales on E_{auto} determinations, which is beyond the scope of this study and requires independent retrieval techniques.

Acknowledgements

The ground-based measurements were obtained from the Atmospheric Radiation Measurement (ARM) Program sponsored by the U.S. Department of Energy (DOE) Office of Energy Research, Office of Health and Environmental Research, and Environmental Sciences

Division. The data can be downloaded from http://www.archive.arm.gov/. This research was supported by the DOE CESM project under grant DE-SC0014641 at the University of Arizona through subaward from University of Maryland at Baltimore County, and the NSF project under grant AGS-1700728 at University of Arizona. We thank Dr. Yangang Liu at Brookhaven National Laboratory for insightful comments and Ms. Casey E. Oswant at the University of Arizona for proof reading the manuscript.

References

Ackerman, A. S., Kirkpatrick, M. P., Stevens, D. E., and Toon, O. B.: The impact of humidity above stratiform clouds on indirect aerosol climate forcing, Nature, 432, 1014–1017, 2004.

Ahlgrimm, M., and Forbes, R.: Improving the Representation of Low Clouds and Drizzle in the ECMWF Model Based on ARM Observations from the Azores, J. Clim., doi: 10.1175/MWR-D-13-00153.1, 2014.

Albrecht, B. A.: Aerosols, cloud microphysics, and fractional cloudiness, Science, 245, 1227–1231, 1989.

Austin, P., Wang, Y., Kujala, V., and Pincus, R.: Precipitation in Stratocumulus Clouds: Observational and Modeling Results, J. Atmos. Sci., 52, 2329–2352, doi:10.1175/1520-0469(1995)052<2329:PISCOA>2.0.CO;2, 1995.

Bai, H., Gong, C., Wang, M., Zhang, Z., and L'Ecuyer, T.: Estimating precipitation susceptibility in warm marine clouds using multi-sensor aerosol and cloud products from A-Train satellites, Atmos. Chem. Phys., 18, 1763-1783, https://doi.org/10.5194/acp-18-1763-2018, 2018.

Barker H. W., Wiellicki B.A., Parker L.: A parameterization for computing grid-averaged solar fluxes for inhomogeneous marine boundary layer clouds. Part II: Validation using satellite data. J. Atmos. Sci. 53: 2304–2316, 1996.

Beheng, K. D.: A parameterization of warm cloud microphysical conversion processes, Atmos. Res., 33, 193-206, 1994.

Bony, S., and Dufresne, J.-L.: Marine boundary layer clouds at the heart of tropical cloud feedback uncertainties in climate models, Geophys. Res. Lett., 32, L20806, doi:10.1029/2005GL023851, 2005.

Boutle, I. A., Abel, S. J., Hill, P. G., and Morcrette, C. J.: Spatial variability of liquid cloud and rain: Observations and microphysical effects. Quart. J. Roy. Meteor. Soc., 140, 583–594, doi:10.1002/qj.2140, 2014.

Chen, T., Rossow, W. B., and Zhang, Y.: Radiative Effects of Cloud-Type Variations, J. Clim., 13, 264–286, 2000.

Cheng, A., and Xu. K.-M.: A PDF-based microphysics parameterization for simulation of drizzling boundary layer clouds, J. Atmos. Sci., 66, 2317–2334, doi:10.1175/2009JAS2944.1, 2009.

Dong, X., Minnis, P., Ackerman, T. P., Clothiaux, E. E., Mace, G. G., Long, C. N., and Liljegren, J. C.: A 25-month database of stratus cloud properties generated from ground-based measurements at the ARM SGP site, J. Geophys. Res., 105, 4529-4538, 2000.

Dong, X., Xi, B., Kennedy, A., Minnis, P. and Wood, R.: A 19-month Marine Aerosol-Cloud_Radiation Properties derived from DOE ARM AMF deployment at the Azores: Part I: Cloud Fraction and Single-layered MBL cloud Properties, J. Clim., 27, doi:10.1175/JCLI-D-13-00553.1, 2014a.

Dong, X., Xi, B., and Wu, P.: Investigation of Diurnal Variation of MBL Cloud Microphysical Properties at the Azores, J. Clim., 27, 8827-8835, 2014b.

Atmos. Chem. Phys. Discuss., https://doi.org/10.5194/acp-2018-499
Manuscript under review for journal Atmos. Chem. Phys.
Discussion started: 19 June 2018

Hahn, C. and Warren, S.: A gridded climatology of clouds over land (1971–96) and ocean (1954–97) from surface observations worldwide, Numeric Data Package NDP-026E ORNL/CDIAC-153, CDIAC, Department of Energy, Oak Ridge, Tennessee, 2007.

Hartmann, D. L., Ockert-Bell, M. E., and Michelsen, M. L.: The Effect of Cloud Type on Earth's Energy Balance: Global Analysis, J. Climate, 5, 1281–1304, https://doi.org/10.1175/15200442(1992)005<1281:TEOCTO>2.0.CO;2, 1992.

Hartmann, D. L. and Short, D. A.: On the use of earth radiation budget statistics for studies of clouds and climate, J. Atmos. Sci., 37, 1233–1250, doi:10.1175/1520-0469(1980)037<1233:OTUOER>2.0.CO;2, 1980.

Houghton, J. T., Ding, Y., Griggs, D.J., Noguer, M., van der Linden, P.J., Dai, X., Maskell, K., and Johnson, C.A.: Climate Change: The Scientific Basis, Cambridge University Press, 881 pp, 2001.

Jess, S.: Impact of subgrid variability on large-scale precipitation formation in the climate model ECHAM5, PhD thesis, Dep. of Environ. Syst. Sci., ETH Zurich, Zurich, Switzerland, 2010.

Jiang, J., Su, H., Zhai, C., Perun, V. S., Del Genio, A., Nazarenko, L. S., Donner, L. J., Horowitz, Seman, L., Cole, C., J., Gettelman, A., Ringer, M. A., Rotstayn, L., Jeffrey, S., Wu, T., Brient, F., Dufresne, J-L., Kawai, H., Koshiro, T., Watanabe, M., LÉcuyer, T. S., Volodin, E. M., Iversen, Drange, T., H., Mesquita, M. D. S., Read, W. G., Waters, J. W., Tian, B., Teixeira, J., and Stephens, G. L.: Evaluation of cloud and water vapor simulations in CMIP5 climate models using NASA ''A-train'' satellite observations, J. Geophys. Res., 117, D14105, doi:10.1029/2011JD017237, 2012.

Kessler, E.: On the distribution and continuity of water substance in atmospheric circulations, Met. Monograph 10, No. 32, American Meteorological Society, Boston, USA, 84 pp., 1969.

Atmos. Chem. Phys. Discuss., https://doi.org/10.5194/acp-2018-499
Manuscript under review for journal Atmos. Chem. Phys.
Discussion started: 19 June 2018

Khairoutdinov, M. and Kogan, Y.: A New Cloud Physics Parameterization in a Large-Eddy Simulation Model of Marine Stratocumulus, Mon. Wea. Rev.,128, 229-243, 2000.

Kooperman, G. J., Pritchard, M. S., Ghan, S. J., Wang, M., Somerville, R. C., and Russell, L. M.: Constraining the influence of natural variability to improve estimates of global aerosol indirect effects in a nudged version of the Community Atmosphere Model 5, J. Geophys. Res., 117, D23204, https://doi.org/10.1029/2012JD018588, 2012.

Larson, V. E., Nielsen, B. J., Fan, J., and Ovchinnikov, M.: Parameterizing correlations between hydrometeor species in mixed-phase Arctic clouds, J. Geophys. Res., 116, D00T02, doi:10.1029/2010JD015570, 2011.

Larson, V. E., and Griffin, B. M.: Analytic upscaling of a local microphysics scheme. Part I: Derivation. Quart. J. Roy. Meteor. Soc., 139, 46–57, 2013.

Lebsock, M. D., Morrison, H., and Gettelman, A.: Microphysical implications of cloud-precipitation covariance derived from satellite remote sensing, J. Geophys. Res.-Atmos., 118, 6521–6533, https://doi.org/10.1002/jgrd.50347, 2013.

Leon, D. C., Wang, Z., and Liu, D.: Climatology of drizzle in marine boundary layer clouds based on 1 year of data from CloudSat and Cloud-Aerosol Lidar and Infrared Pathfinder Satellite Observations (CALIPSO), J. Geophys. Res., 113, D00A14, doi:10.1029/2008JD009835, 2008.

Liljegren, J. C., Clothiaux, E. E., Mace, G. G., Kato, S., and Dong, X.: A new retrieval for cloud liquid water path using a ground-based microwave radiometer and measurements of cloud temperature, J. Geophys. Res., 106, 14,485-14,500, 2001.

Liu, Y. and Daum, P. H.: Parameterization of the autoconversion process, Part I: Analytical formulation of the Kessler-type parameterizations, J. Atmos. Sci., 61, 1539–1548, 2004.

Liu, Y., Daum, P. H., and McGraw, R.: Parameterization of the autoconversion process. Part II: Generalization of Sundqvist-type parameterizations, J. Atmos. Sci., 63, 1103–1109, 2006a.

Atmospheric Chemistry and Physics Discussions

Liu, Y., Daum, P. H., McGraw, R., Miller, M.: Generalized threshold function accounting for effect of relative dispersion on threshold behavior of autoconversion process. Geophys. Res. Lett., 33, L11804, 2006b.

Lohmann, U. and Feichter, J.: Global indirect aerosol effects: a review, Atmos. Chem. Phys., 5, 715–737, doi:10.5194/acp-5-715-2005, 2005.

Morrison, H. and Gettelman, A.: A new two-moment bulk stratiform cloud microphysics scheme in the Community Atmosphere Model, version 3 (CAM3). Part I: Description and numerical tests, J. Climate, 21, 3642–3659, 2008.

Nam, C., and Quaas, J.: Evaluation of clouds and precipitation in the ECHAM5 general circulation model using CALIPSO and CloudSat satellite data, J. Clim., 25, 4975–4992, doi:10.1175/JCLI-D-11-00347.1, 2012.

O'Connor, E. J., Hogan, R. J., and Illingworth, A. J.: Retrieving stratocumulus drizzle parameters using Doppler radar and lidar, J. of Applied Meteorol., 44, 14-27, 2005.

Pincus, R., McFarlane, S. A., and Klein, S. A.: Albedo bias and the horizontal variability of clouds in subtropical marine boundary layers: Observations from ships and satellites, J. Geophys. Res., 104, 6183–6191, doi:10.1029/1998JD200125, 1999.

Pincus, R., and Klein, S. A.: Unresolved spatial variability and microphysical process rates in large-scale models. J. Geophys. Res., 105D, 27 059–27 065, 2000.

Quaas, J., Ming, Y., Menon, S., Takemura, T., Wang, M., Penner, J. E., Gettelman, A., Lohmann, U., Bellouin, N., Boucher, O., Sayer, A. M., Thomas, G. E., McComiskey, A., Feingold, G., Hoose, C., Kristjánsson, J. E., Liu, X., Balkanski, Y., Donner, L. J., Ginoux, P. A., Stier, P., Grandey, B., Feichter, J., Sednev, Bauer, S. E., Koch, D., Grainger, R. G., Kirkevåg, A., Iversen, T., Seland, Ø., Easter, R., Ghan, S. J., Rasch, P. J., Morrison, H., Lamarque, J.-F., Iacono, M. J., Kinne, S., and Schulz, M.: Aerosol indirect effects – general circulation model intercomparison and evaluation with satellite data, Atmos. Chem. Phys., 9, 8697–8717, https://doi.org/10.5194/acp-9-8697-2009, 2009.

Randall, D. A., Coakley, J. A., Fairall, C. W., Knopfli, R. A., and Lenschow, D. H.: Outlook for research on marine subtropical stratocumulus clouds. Bull. Amer. Meteor. Soc., 65, 1290–1301, 1984.

Rémillard, J., Kollias, P., Luke, E., and Wood, R.: Marine Boundary Layer Cloud Observations in the Azores, J. Climate, 25, 7381–7398, doi: http://dx.doi.org/10.1175/JCLI-D-11-00610.1, 2012.

Slingo, A.: Sensitivity of the Earth's radiation budget to changes in low clouds, Nature, 343, 49–51, https://doi.org/10.1038/343049a0, 1990.

Song, H., Zhang, Z., Ma, P.-L., Ghan, S. J., and Wang, M.: An Evaluation of Marine Boundary Layer Cloud Property Simulations in the Community Atmosphere Model Using Satellite Observations: Conventional Subgrid Parameterization versus CLUBB, J. Clim., doi:10.1175/JCLI-D-17-0277.1, 2018.

Stanfield, R., Dong, X., Xi, B., Gel Genio, A., Minnis, P., and Jiang, J.: Assessment of NASA GISS CMIP5 and post CMIP5 Simulated Clouds and TOA Radiation Budgets Using Satellite Observations: Part I: Cloud Fraction and Properties, J. Clim., doi:10.1175/JCLI-D-13-00588.1, 2014.

Tripoli, G. J. and Cotton, W. R.: A numerical investigation of several factors contributing to the observed variable intensity of deep convection over South Florida., J. Appl. Meteorol., 19, 1037–1063, 1980.

Troyan, D.: Merged Sounding Value-Added Product, Tech. Rep., DOE/SC-ARM/TR-087, 2012.

Wang, M., Ghan, S., Liu, X., L'Ecuyer, T. S., Zhang, K., Morrison, H., Ovchinnikov, M., Easter, R., Marchand, R., Chand, D., Qian, Y., and Penner, J. E.: Constraining cloud lifetime effects of aerosols using A-Train satellite observations, Geophys. Res. Lett., 39, L15709, https://doi.org/10.1029/2012GL052204, 2012.

Warren, S. G., Hahn, C. J., London, J., Chervin, R. M., and Jenne, R.: Global distribution of total cloud cover and cloud type amount over land, Tech. Rep. Tech. Note TN-317 STR, NCAR, 1986.

Warren, S. G., Hahn, C. J., London, J., Chervin, R. M., and Jenne, R.: Global distribution of total cloud cover and cloud type amount over land, Tech. Rep. Tech. Note TN-317 STR, NCAR, 1988.

Weber, T., and Quaas, J.: Incorporating the subgrid-scale variability of clouds in the autoconversion parameterization using a PDF-scheme, J. Adv. Model. Earth Syst., 4, M11003, doi:10.1029/2012MS000156, 2012.

Wielicki, B. A., Cess, R. D., King, M. D., Randall, D. A., and Harrison, E. F.: Mission to planet Earth: Role of clouds and radiation in climate, Bull. Amer. Meteor. Soc., 76, 2125–2153, doi:10.1175/1520-0477(1995)076,2125:MTPERO.2.0.CO;2, 1995.

Wood, R., Field, P. R., and Cotton, W. R.: Autoconversion rate bias in stratiform boundary layer cloud parameterization. Atmos. Res., 65, 109–128, 2002.

Wood, R.: Drizzle in stratiform boundary layer clouds. Part I: Vertical and horizontal structure, J. Atmos. Sci., 62, 3011–3033, 2005a.

Wood, R.: Drizzle in stratiform boundary layer clouds. Part II: Microphysical aspects, J. Atmos. Sci., 62, 3034–3050, 2005b.

Wood, R. and Hartmann, D.: Spatial variability of liquid water path in marine low cloud: The importance of mesoscale cellular convection, J. Climate, 19, 1748–1764, 2006.

Wood, R.: Cancellation of aerosol indirect effects in marine stratocumulus through cloud thinning. J. Atmos. Sci., 64, 2657–2669, 2007.

Wood, R.: Stratocumulus Clouds, Mon. Wea. Rev., 140, 2373–2423. doi: http://dx.doi.org/10.1175/MWR-D-11-00121.1, 2012.

Atmos. Chem. Phys. Discuss., https://doi.org/10.5194/acp-2018-499
Manuscript under review for journal Atmos. Chem. Phys.
Discussion started: 19 June 2018

Wood, R., Wyant, M., Bretherton, C. S., Rémillard, J., Kollias, P., Fletcher, J., Stemmler, J., deSzoeke, S., Yuter, S., Miller, M., Mechem, D., Tselioudis, G., Chiu, C., Mann, J., O'Connor, E., Hogan, R., Dong, X., Miller, M., Ghate, V., Jefferson, A., Min, Q., Minnis, P., Palinkonda, R., Albrecht, B., Luke, E., Hannay, C., Lin, Y.: Clouds, Aerosol, and Precipitation in the Marine Boundary Layer: An ARM Mobile Facility Deployment, Bull. Amer. Meteorol. Soc., doi: http://dx.doi.org/10.1175/BAMS-D-13-00180.1, 2015.

Wu, P., Dong, X. and Xi, B.: Marine boundary layer drizzle properties and their impact on cloud property retrieval, Atmos. Meas. Tech., 8, 3555–3562. doi: 10.5194/amt-8-3555-2015, 2015.

Wu, P., Dong, X., Xi, B., Liu, Y., Thieman, M., and Minnis, P.: Effects of environment forcing on marine boundary layer cloud-drizzle processes, J. Geophys. Res. Atmos., 122, 4463–4478, doi:10.1002/2016JD026326, 2017.

Xie, X., and Zhang, M.: Scale-aware parameterization of liquid cloud inhomogeneity and its impact on simulated climate in CESM, J. Geophys. Res. Atmos., 120, 8359–8371, doi:10.1002/2015JD023565, 2015.

Yoo, H., and Li, Z.: Evaluation of cloud properties in the NOAA/NCEP Global Forecast System using multiple satellite products. Climate Dyn., 39, 2769–2787, doi:10.1007/s00382-012-1430-0, 2012.

Yoo, H., and Li, Z., Hou, Y.-T., Lord, S., Weng, F., and Barker, H. W.: Diagnosis and testing of low-level cloud parameterizations for the NCEP/GFS using satellite and ground-based measurements. Climate Dyn., 41, 1595–1613, doi:10.1007/s00382-013-1884-8, 2013.

Zhang, J., Lohmann, U., and Lin, B.: A new statistically based autoconversion rate parameterization for use in large-scale models. J. Geophys. Res., 107, 4750, doi:10.1029/2001JD001484, 2002.

Atmos. Chem. Phys. Discuss., https://doi.org/10.5194/acp-2018-499
Manuscript under review for journal Atmos. Chem. Phys.
Discussion started: 19 June 2018

Table 1. The parameters of autoconversion and accretion formulations for four parameterizations.

	A	$a1$	$a2$	B	b
Khairoutdinov and Kogan (2000)	1350	2.47	-1.79	67	1.15
Liu and Daum (2004)	$1.3 \times 10\beta_6^6$, where $\beta_6^6 = [(r_v + 3)/r_v]^2$, r_v is mean volume radius. modification was made by Wood (2005b)	3	-1	N/A	N/A
Tripoli and Cotton (1980)	3268	7/3	-1/3	1	1
Beheng (1994)	3×10^{34} for $N_c < 200$ cm^{-3} 9.9 for $N_c > 200$ cm^{-3}	4.7	-3.3	1	1

Atmos. Chem. Phys. Discuss., https://doi.org/10.5194/acp-2018-499
Manuscript under review for journal Atmos. Chem. Phys.
Discussion started: 19 June 2018

Atmospheric Chemistry and Physics
Discussions

Table 2. Autoconversion (left) and accretion (right) enhancement factors in different boundary layer conditions (LTS > 18 K for stable, LTS < 13.5 K for unstable and LTS within 13.5 and 18 K for mid-stable) and in different LWP regimes (LWP ≤ 75 g m^{-2} for non-precipitating and LWP > 75 g m^{-2} for precipitating).

LTS (K)	LWP ≤ 75 g m^{-2}	LWP > 75 g m^{-2}
> 18	2.31/1.40	2.58/1.49
(13.5, 18)	2.56/1.43	2.98/1.63
< 13.5	4.15/1.51	6.17/1.70

Atmos. Chem. Phys. Discuss., https://doi.org/10.5194/acp-2018-499
Manuscript under review for journal Atmos. Chem. Phys.
Discussion started: 19 June 2018

Table 3. Autoconversion and accretion enhancement factors (E_{auto} and E_{accr}) for the parameterizations in Table 1 except the Khairoutdinov and Kogan (2000) scheme. The values 2-hr and 5-hr interval averages.

	E_{auto}		E_{accr}	
	2-hour	5-hour	2-hour	5-hour
Liu and Daum (2004)	3.76	4.20	N/A	N/A
Tripoli and Cotton (1980)	2.55	2.71	1.25	1.31
Beheng (1994)	6.73	5.00	1.25	1.31

Atmos. Chem. Phys. Discuss., https://doi.org/10.5194/acp-2018-499
Manuscript under review for journal Atmos. Chem. Phys.
Discussion started: 19 June 2018

Atmospheric Chemistry and Physics
Discussions

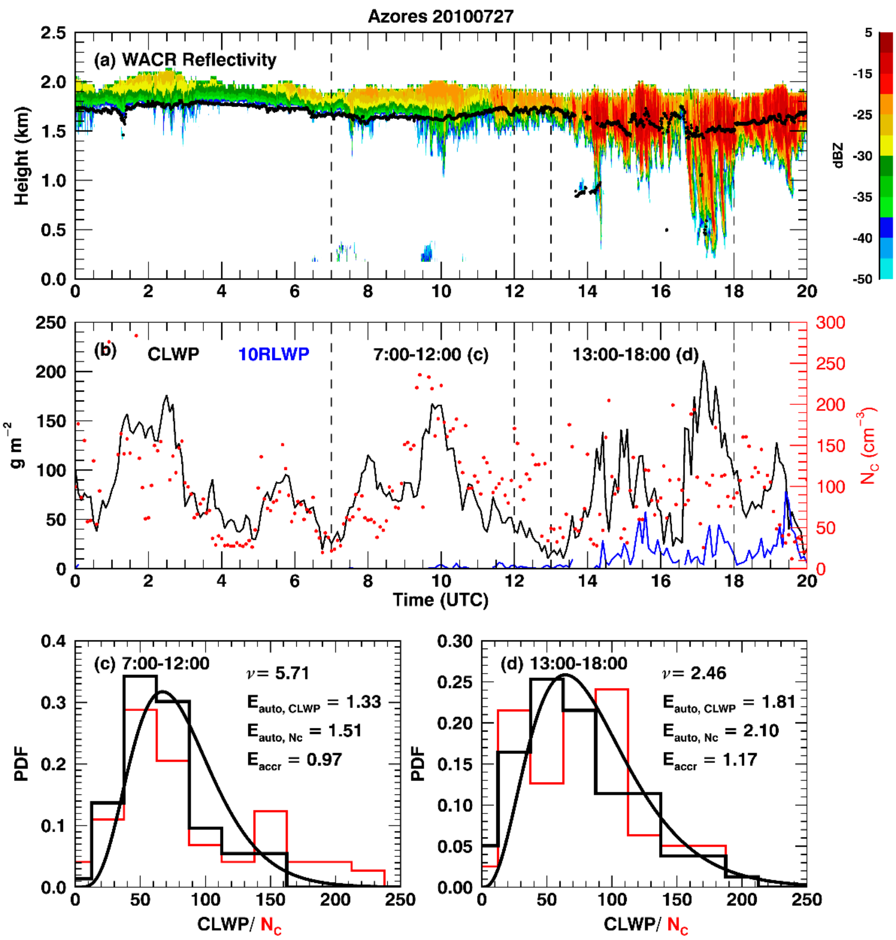

Figure 1. Observations and retrievals over Azores on 27 July 2010. (a) W-band ARM cloud radar (WACR) reflectivity (contour) superimposed with cloud-base height (black dots). (b) Cloud and rain (×10) liquid water path (CLWP in black and 10RLWP in blue), red dots are the retrieved cloud droplet number concentration (N_c). Dashed lines represent two time periods with similar mean-CLWP but different distributions as shown by black step lines in (c) and (d). Black curved lines in (c) and (d) are fitted gamma distributions with the corresponding shape parameter (ν) shown on the upper right. Red step lines show N_c distributions. The calculated autoconversion ($E_{auto,\ CLWP}$ from CLWP and $E_{auto,\ Nc}$ from N_c) and accretion (E_{accr}) enhancement factors are also shown.

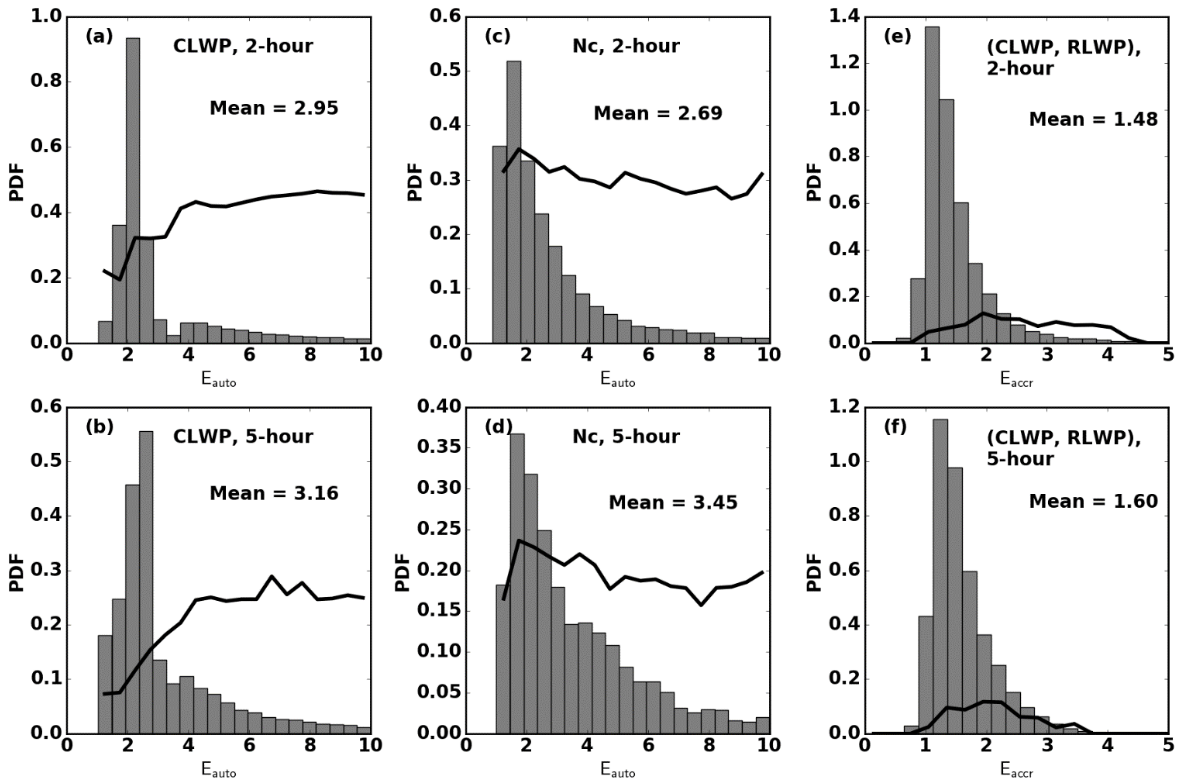

Figure 2. Probability density functions (PDFs) of autoconversion (a - d) and accretion (e - f) enhancement factors calculated from CLWP (a-b), N_c (c-d), and the covariance of CLWP and rain LWP (RLWP) (e-f). First two rows show the results from 2-hr and 5-hr intervals, respectively, with their average values. Black lines represent precipitation frequency in each bin in (a)-(d) and the ratio of RLWP to CLWP in (e)-(f).

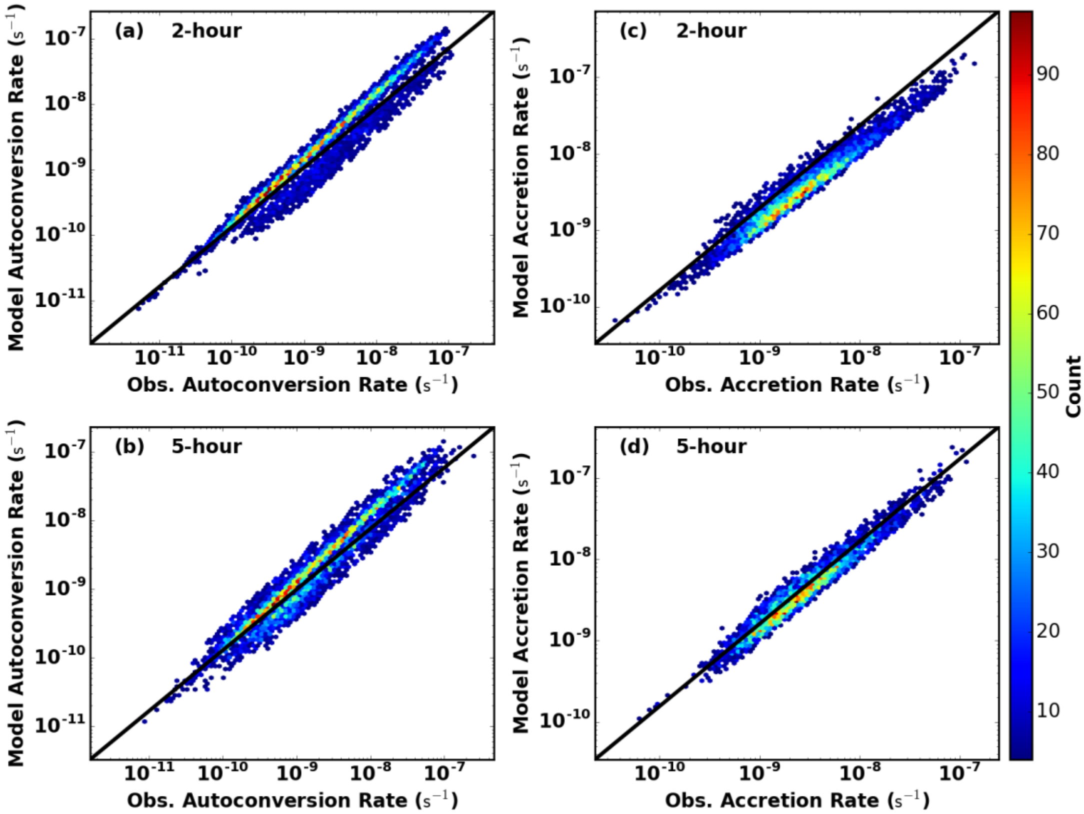

Figure 3. Comparison of autoconversion (a-b) and accretion (c-d) rates derived from observations (x-axis) and from model (y-axis). Results are for 2-hr (a and c) and 5-hr intervals. Colored dots represent joint number densities.

Atmos. Chem. Phys. Discuss., https://doi.org/10.5194/acp-2018-499
Manuscript under review for journal Atmos. Chem. Phys.
Discussion started: 19 June 2018

Atmospheric Chemistry and Physics
Open Access
Discussions

688

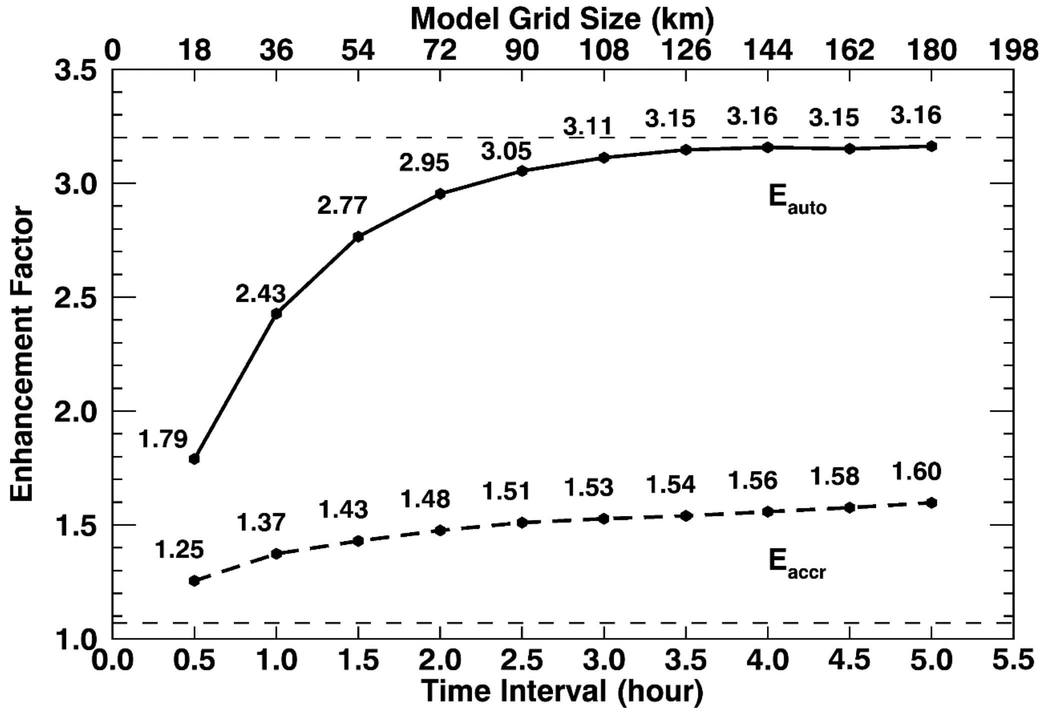

689

690 **Figure 4. Autoconversion (solid dot line) and accretion (dashed dot line) enhancement**
691 **factors as a function of time interval (of surface observations). The model grid box sizes**
692 **on the top X-axis are calculated using a horizontal wind of 10 m s^{-1}. The two dashed**
693 **lines show the constant values of autoconversion (3.2) and accretion (1.07) enhancement**
694 **factors used in GCMs.**

695

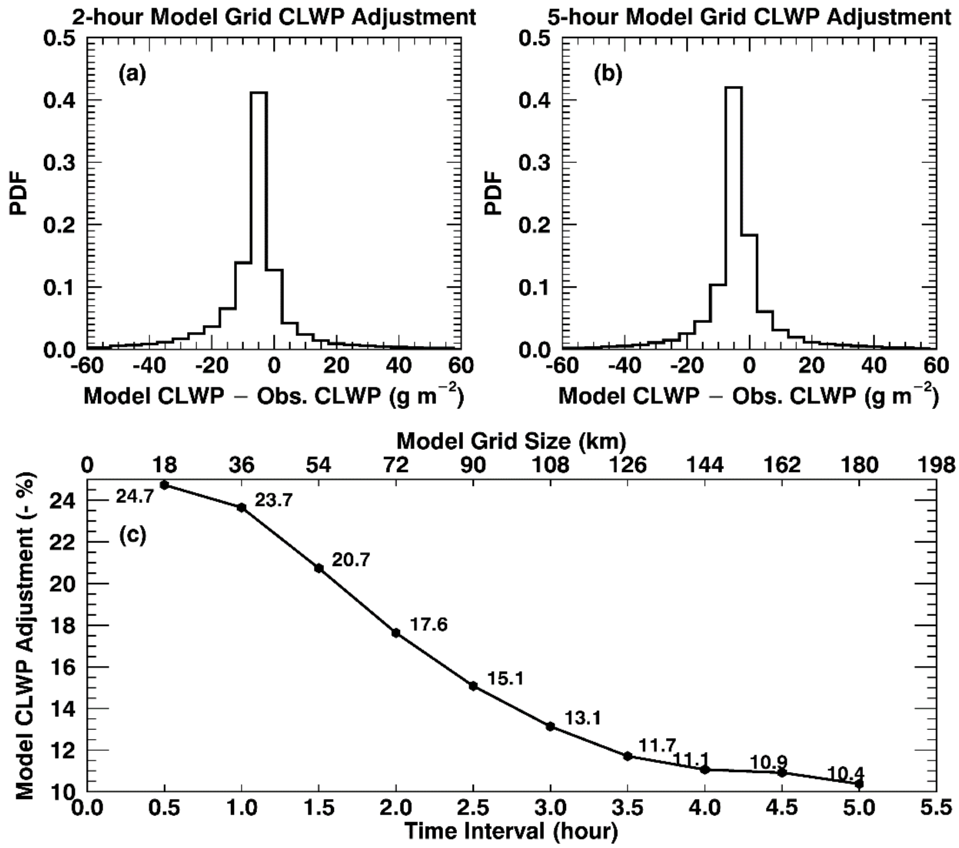

Figure 5. CLWPs needed for models to adjust to reach the same autoconversion rate as observations for (a) 2-hour and (b) 5-hour intervals. Positive biases represent increased CLWPs required in models and negative biases mean decreased CLWPs. The average percentages of adjustments for different model grid sizes are shown in panel (c) and note that the percentages in the vertical axis are negative.